

Engineered biochar-metal oxide nanocomposites for targeted dye remediation in textile wastewater

Faisal Mehmood¹, Muhammad Nadeem², Obid Tursunov^{3,4,5*} , Ren Sihao¹, Yongkun Fu¹, Renjie Dong^{1,6,7}, Bakhtiyor Meliyev⁸, Makhsudjon Ochilov⁸, Gayrat Egamnazarov⁸, Yuguang Zhou^{1,6,7*}

¹ Bioenergy and Environment Science & Technology Laboratory, College of Engineering, China Agricultural University, Beijing 100083, China

² Beijing Key Laboratory of Farmland Soil Pollution Prevention and Remediation and College of Resources and Environmental Sciences, China Agricultural University, Beijing 100193, China

³ Department of Power Supply and Renewable Energy Sources, National Research University TIAME, Tashkent 100000, Uzbekistan

⁴ College of Mechanical and Electrical Engineering, Shihezi University, Beisi Road, Shihezi, Xinjiang 832000, China

⁵ Department of Ecology and Labor Protection, Jizzakh Polytechnic Institute, Jizzakh 130100, Uzbekistan

⁶ Key Laboratory of Clean Production and Utilization of Renewable Energy, Ministry of Agriculture and Rural Affairs, China, Beijing 100083, China

⁷ National Center for International Research of BioEnergy Science and Technology, Ministry of Science and Technology, Beijing 100083, China

⁸ Jizzakh Polytechnic Institute, Jizzakh 130100, Uzbekistan

* Corresponding author's email: obidtursunov@gmail.com; zhouyg@cau.edu.cn

ABSTRACT

The global textile industry releases nearly 280,000 tons of synthetic dyes each year, generating persistent pollutants that disrupt aquatic ecosystems as well as pose carcinogenic and mutagenic risks. Conventional treatment technologies such as activated carbon adsorption, advanced oxidation processes, and biological degradation often fail to address the complexity of real industrial effluents. This review critically evaluated engineered biochar metal oxide nanocomposites (BMO-NCs) as emerging dual-functional materials that integrate adsorption with photocatalytic degradation for targeted dye removal. The authors highlighted how the tunable surface chemistry, hierarchical porosity, and electronic conductivity of biochar synergize with metal-oxide-driven reactive oxygen species ($\bullet\text{OH}$, $\bullet\text{O}_2^-$, h^+) to enhance degradation pathways. While laboratory studies frequently report >95% dye removal, real-wastewater conditions such as fluctuating pH, high salinity, and competing contaminants significantly reduce performance. To bridge this gap, key research priorities were identified, including mechanistic validation of ROS via in-situ ESR, LC-MS tracking of degradation intermediates, long-term regeneration and metal-leaching assessments, and standardized testing protocols for industrial effluents. This review provided design principles for scalable, safe, and circular-economy-aligned BMO-NCs, underscoring their potential contribution to Sustainable Development Goal 6.

Keywords: biochar-metal oxide nanocomposites, textile wastewater treatment, adsorption-photocatalysis synergy, reactive oxygen species, synthetic dye degradation.

INTRODUCTION

The rising global demand for textiles, printing, leather, paint, food, pharmaceuticals, and other industrial processes have led to the generation

of vast level of contaminated water with synthetic organic dyes (Oguanobi et al., 2025; Periyasamy, 2024; Uddin, 2021). Globally, an estimated 700,000 tons of synthetic dyes are generated annually, with approximately 280,000 tons released

into effluents, making dyes one of the prominent classes of industrial pollutants (Sahu and Poler, 2024; Singh et al., 2024). These dyes are designed for widespread use, contributing to their persistence in aquatic systems. Their presence reduces aesthetic quality as well as poses severe eco-toxicological and health hazards (Rajak et al., 2024). Figure 1 summarizes the principal industrial sources of dye pollution (e.g., textile, leather, printing, paper and pharmaceutical sectors) and the main pathways by which dye-laden effluents impair aquatic ecosystems, reduce water quality, and create human-health risks. The organic dyes, often associated with aromatic structures, reduce light and oxygen penetration, which negatively affects aquatic ecosystems, photosynthesis, and microbial activity (Kumari, 2024; Mukherjee et al., 2024). Furthermore, certain synthetic dyes exhibit carcinogenic, mutagenic, and other adverse health impacts in humans, including cancer and respiratory infections, demand the urgent need for effective remediation strategies before discharge into water bodies (Kumari, 2024; Ramamurthy et al., 2024).

Addressing this critical environmental issue requires innovative remediation technologies that are both effective and sustainable. Numerous techniques, such as, spanning physicochemical, and biological method working on removal of organic dyes from wastewater (N Lotha et al., 2024; Sornaly et al., 2024). Adsorption methods, such as activated carbon, efficiently remove dyes and are simple to use; however, their cost, limited sustainability, and reduced effectiveness against complex dye mixtures restricted their practical applications (Akinnike et al., 2024). Advanced oxidation processes (AOPs), such as photocatalysis, generate reactive oxygen species ($\cdot\text{OH}$, h^+ and $\cdot\text{O}_2^-$) that efficiently degrade pollutants. However, their practical application is limited by high energy requirements, complex setups, and low effectiveness in treating real effluents (Iqbal et al., 2024). Biological methods, while environmentally friendly, often struggle with the recalcitrant nature and structural complexity of many synthetic dyes, which are inherently resistant to biodegradation (Sharma et al., 2024). Despite these advancements, conventional wastewater treatment plants often failed to remove persistent organic dyes, highlighting the need for more robust and effective treatment technologies.

Engineered biochar based nanocomposites (NCs), particularly those incorporating metal

oxides, constitute an emerging and sustainable solution for dye removal (Ahmad et al., 2024; Damahé et al., 2024). Pyrolysis of low-cost waste biomass yield biochar, a material characterized by a high surface area, significant porosity, and tunable surface chemistry. The incorporation of metal oxide can further functionalize biochar, creating the composites capable of the simultaneous adsorption and photocatalytic degradation of pollutants (Awais Ahmad et al., 2024; Attiqah Ahmad et al., 2024). This integration improves surface charge and pH tune-ability, allowing for efficient wastewater management (Kumar et al., 2025). These synergistic properties of metal oxide biochar NCs enable them to produce next-generation materials for integrated dye remediation. The synergistic action of adsorption and photocatalytic degradation allows these NCs to efficiently remove pollutants from complex wastewater, surpassing the performance of conventional treatments (Haleem et al., 2023). Recent studies have demonstrated that the biochar-supported ZnO composites effectively degrade organic dyes such as methylene blue and rhodamine B. The photocatalytic activity is significantly enhanced by the incorporation of ZnO, with biochar providing adsorption sites for the dye molecules (Kaur, 2022). Another study demonstrated the preparation of peanut shell biochar-loaded $\text{TiO}_2/\text{Ce}-\text{C}_3\text{N}_4$ heterojunctions, significantly enhancing photocatalytic activity for methylene blue (MB) degradation under visible light. The composite achieved 100% MB removal after 30 minutes of adsorption and 7 minutes of irradiation, with a rate constant 19 times higher than $\text{Ce}-\text{C}_3\text{N}_4$ and 16 times higher than TiO_2 . The synergistic adsorption-photocatalytic effect and reduced band gap energy contributed to efficient pollutant removal and excellent stability (Li et al., 2024). A similar study synthesized biochar-supported copper oxide composite (BC-CuO) to activate peroxymonosulfate (PMS) for treating highly saline wastewater. The BC-CuO/PMS system achieved rapid removal of various pollutants, including Methylene Blue, Rhodamine B, and Ciprofloxacin, with efficiencies up to 100% under highly saline conditions. The degradation process was dominated by singlet oxygen ($^1\text{O}_2$), and the results suggest that BC-CuO/PMS is a promising technique for removing organic pollutants from complex and saline wastewater systems (Li et al., 2020).

In this study, dye removal using biochar-metal oxide nanocomposites (BMO-NCs) was

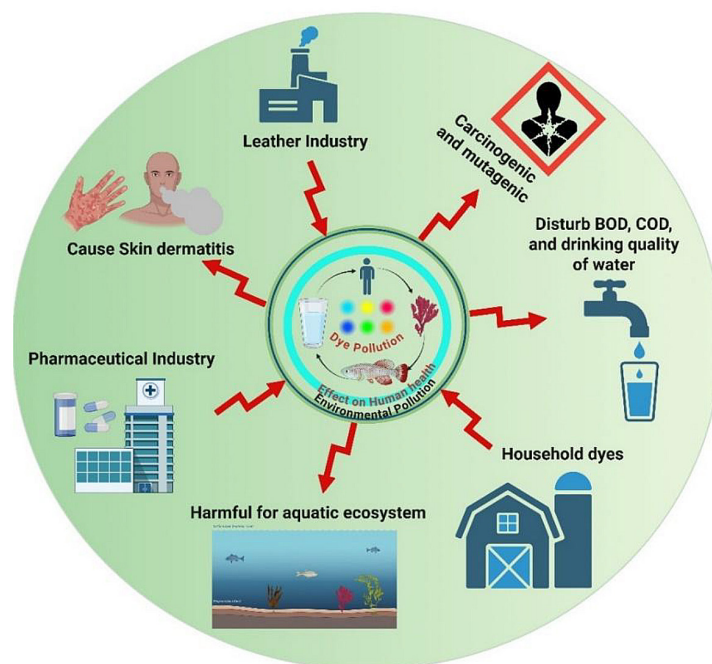


Figure 1. Major industrial sources of dye pollution and their associated environmental and human health impacts, including aquatic ecosystem degradation, water-quality deterioration, skin disorders, and carcinogenic risk

comprehensively examined. Nevertheless, a significant knowledge gap persists between lab scale advancement and practical implementation at the industrial level. Previous studies lack an in depth analysis of real-world complexities, such as dye mixtures, varying pH, salinity, co-contaminants, and comprehensive economic or lifecycle assessments essential for long-term feasibility (Mogashane et al., 2024; Hellal et al., 2025). Future research is required to validate the scalability, regeneration potential, and cost effectiveness of emerging compounds. Unlike conventional reviews focused on synthetic dye solutions, this paper emphasized material performance under real wastewater conditions. The design, mechanisms, and efficacy of BMC-NCs, were critically evaluated with a focus on their practical application in industrial wastewater treatment.

CHEMISTRY-GUIDED DESIGN

Chemistry-guided design serves as the foundational framework for engineering biochar metal oxide nanocomposites (BMO-NCs) with high selectivity, durability, and efficiency for dye remediation under complex wastewater conditions (Amdeha, 2024; Aslam et al., 2024). The performance of BMO-NCs is governed by the interplay between biochar surface chemistry as well as the

electronic and catalytic properties of the incorporated metal oxides (Amdeha, 2024; Zheng et al., 2025). Together, these features define how the composite interacts with cationic, anionic, and structurally diverse azo dyes. At the molecular scale, the adsorption of ionizable dyes in aqueous media is primarily governed by electrostatic interactions, which are strongly modulated by solution pH relative to the point of zero charge of the material (pH_{pzc}) (Sayed et al., 2025; Strebel et al., 2024). Conversely, protonation at $pH < pH_{pzc}$ ($\equiv C-OH + H^+ \rightarrow \equiv C-OH_2^+$) generates a positively charged surface that enhances the binding of sulfonated anionic dyes like Congo Red and Eriochrome Black T (Oluwasina et al., 2024). Such charge-governed behavior is substantiated by zeta potential measurements, surface titrations, and density functional theory (DFT) insights, showing how protonation states alter surface electron density and binding affinity (Qin et al., 2024; Y. Zhang et al., 2024). In realistic textile effluents, the charge behavior of BMO-NCs is governed not only by pH_{pzc} but also by electrical-double-layer (EDL) structure and Donnan ion partitioning. Elevated ionic strength collapses the Debye length and compresses the diffuse layer, attenuating the effective surface potential and diminishing long-range electrostatic attraction a trend consistently observed through reduced magnitude of zeta

potential and lower adsorption of charged dyes at high salinity (George et al., 2024; Kar et al., 2025; Wu, 2022). At high electrolyte concentrations, Stern-layer charge compensation becomes significant: specifically, adsorbing ions (e.g., Ca^{2+} , Mg^{2+} , Cl^- , SO_4^{2-}) neutralize surface functional groups, suppressing accessible charge sites and reducing chemisorption capacity. Moreover, strong ion pairing (e.g., Na^+ –dye $^-$ or SO_4^{2-} –dye $^+$ complexes) lowers the activity coefficients of ionic dyes, effectively decreasing the fraction of “free” dye available for interaction with active sites. Collectively, EDL compression, Donnan exclusion, Stern-layer compensation, and ion-pairing effects explain the substantial performance disparities observed between deionized laboratory systems and complex saline wastewaters.

Beyond electrostatic attraction, the π – π interactions between the sp^2 -hybridized carbon domains of biochar and aromatic dye rings significantly strengthen the adsorption of cationic dyes, while hydrogen bonding with surface $-\text{OH}$, $-\text{COOH}$, and $-\text{C}=\text{O}$ groups further promotes dye adsorption (Wang et al., 2025). In addition, coordination and Lewis acid base interactions arise when metal centers (e.g. Cu^{2+} , Fe^{3+} , Mn^{3+} , Zn^{2+}) bind electron-rich functional groups on dye molecules (Ahmed et al., 2025). The porous architecture of engineered biochar provides confinement effects and capillary driven pore filling, enabling rapid mass transfer and pre-concentration of pollutants at the catalytic interface. Incorporating metal oxides introduces oxygen vacancies, surface hydroxylation, and tunable redox as well as band-edge properties that strongly affect adsorption and photocatalytic activity (Yang et al., 2025). Oxygen-deficient sites act as electron traps and increase chemisorption, while heterojunction formation between biochar and metal oxides suppresses electron hole recombination and accelerates the generation of reactive oxygen species (Hailili and Gan, 2025). These combined effects significantly amplify the dual-function efficiency of BMO-NCs under visible-light or oxidant-assisted conditions, even in the presence of competing ions and co-contaminants. Chemistry-guided design provides a mechanistic blueprint enabling BMO-NCs to selectively target and efficiently remove cationic dyes, anionic sulfonated dyes, and recalcitrant azo dyes the degradation of which requires both strong adsorption and catalytic bond cleavage. This design philosophy not only rationalizes material performance, but also

provides information on the development of next-generation composites optimized for real industrial wastewater environments. In the following sections, these chemistry-guided principles are further deconstructed into charge-specific design strategies for cationic and anionic dyes, providing a basis for rational tailoring of BMO-NCs for targeted dye remediation.

Charge-specific design strategies

Textile wastewater contains highly conjugated and ionizable dyes that remain mobile due to strong resonance stabilization and hydrophilicity (Periyasamy, 2024; Ran et al., 2024). As a result, the performance of (BMO-NCs) depends not only on porosity or surface area but largely on the electrostatic compatibility between the dye molecules and the engineered surface charge of the composite. Therefore, charge specific design acts as the primary mechanism governing dye recognition, interfacial accumulation, and catalytic activation (Periyasamy, 2024). Surfaces switch between protonated ($-\text{M}-\text{OH}_2^+$, $-\text{NH}_2^+$) and deprotonated ($-\text{M}-\text{O}^-$, $-\text{COO}^-$) states, even a 1–2-unit shift in pH relative to pH_{pzc} may alter adsorption capacity by more than an order of magnitude. This shift modifies electrostatic attraction, reduces competition between protons and dye ions, as well as affects both inner- and outer-sphere complexation pathways (P. Zhang et al., 2024)

ZnO biochar and CuO biochar composites develop negative zeta potentials (-20 to -35 mV) at near-neutral pH, enabling $>95\%$ MB removal through combined electrostatic attraction, π – π stacking, and Lewis base interactions from oxygenated groups on biochar (Ameen et al., 2025; Yadav et al., 2026). Conversely, Mn–CuO@biochar and Fe-modified biochars with high pH_{pzc} values (>5.5) maintain strong positive charge under acidic conditions. These materials achieve $>98\%$ CR and EBT removal due to electrostatic attraction, hydrogen bonding, and Lewis acidic interactions at metal oxide sites (Ullah et al., 2025). In real effluents, competitive ions such as Cl^- and SO_4^{2-} can partially screen electrostatic forces; therefore, maintaining high surface charge density is essential for stable performance under high-ionic-strength conditions (Liu et al., 2025). Charge-specific adsorption also enhances catalytic degradation. Local enrichment of dye molecules at the BMO-NC interface reduces mass-transfer limitations and increases the probability of dye–ROS

interaction (Suthar and Patidar, 2024). Negatively charged surfaces promote O_2 activation and enhance $\bullet O_2^-$ generation, whereas protonated metal oxide sites accelerate H_2O_2 activation and $\bullet OH$ production through Fe^{2+}/Fe^{3+} , Cu^+/Cu^{2+} , and Mn^{3+}/Mn^{4+} redox cycling (Feng et al., 2024; Suthar and Patidar, 2024; Yang et al., 2024). This synergy is especially important for azo dyes, where complete cleavage of the $-N=N-$ bond requires both selective pre-concentration and sustained ROS attack (Oral et al., 2024).

Thus, charge-specific design provides the conceptual framework for achieving selective adsorption, efficient ROS generation, and hybrid adsorption–oxidation pathways. The following subsections translate these principles into targeted strategies for cationic, anionic, and azo dyes, forming a unified design logic for textile wastewater.

Cationic dyes

Cationic dyes, like methylene blue (MB), carry a positive charge in aqueous solutions (Yildirim et al., 2024; Sannino et al., 2024). To effectively remove the dyes through electrostatic attraction, the adsorbent surface should be negatively charged (Attia Ahmad et al., 2024; Ashebir et al., 2024). Moreover, pH significantly influenced the surface charge of an adsorbent link to the point of zero charge (pH_{pzc}) (Adawiyah et al., 2025; Amdeha, 2024). From pH_{pzc} if the pH is increased, the adsorbent surface tend towards negative charge (Oraon et al., 2024), which enhances the electrostatic attraction with positively charge cationic dyes like MB, leading to increased adsorption and degradation efficiencies (Radoor et al., 2024). Studies on $CuO@BSS$ NCs, practical for MB removal, showed their pH_{pzc} was around pH 3.8, and their outer surface charge was negative over a broad pH range above this value (Gomaa et al., 2022). Additionally, if the pH values decrease from point of zero charge (PZC), surface become positive charge due to protonation, causing repulsive forces with cationic dyes and reducing removal efficiency; H^+ ions also compete for active sites at low pH (Ederer et al., 2025; Gomaa et al., 2022). Similarly, another study shows that MB adsorption onto ZnO /biochar is highly pH dependent, with acidic conditions limiting uptake due to H^+ competition, while alkaline conditions enhance electrostatic attraction between the deprotonated biochar surface and cationic MB. As a result, adsorption capacity and removal efficiency

increase sharply with pH and stabilize at higher alkaline values. Similarly, biochar exhibited higher adsorption of MB under alkaline conditions compared to acidic conditions, highlighting the influence solution pH on adsorbent dye interactions (Borthakur et al., 2021; Yan et al., 2024).

For aromatic cationic dyes like MB electrostatic forces and π - π interaction are also crucial for the adsorption (Salahshoori et al., 2024). These interactions occur between graphitic domains present in the biochar structure and aromatic rings in dye molecules (Liang et al., 2024). The degree of aromaticity in the dye molecule plays a crucial role in their interaction with adsorbent. The instant MB from wood biochar removed by potassium hydroxide modified phenol formaldehyde via electrostatic attraction, π - π interactions and pore-filling (Hakami, 2023; Ning et al., 2024) whereas the date palm-derived Fe-modified biochar also removes MB through hydrogen bonding, electrostatic attraction, and π - π interactions (Grabi et al., 2022; Shafiq et al., 2025). Post modification introduces functional groups like hydroxyls and amines to enhance π - π interactions in biochar-based nanocomposites (Guo et al., 2023), as demonstrated in porous ZnO /peanut shell-biochar nanocomposite that achieved high Methylene Blue adsorption (426.44 mg g^{-1}) via π - π and electrostatic mechanism. Figure 2 illustrates the charge-dependent adsorption mechanisms governing the interaction of cationic and anionic dyes with BMO-NC surfaces, emphasizing how pH-driven transitions relative to the pH_{pzc} of the material dictate electrostatic attraction, the π - π interactions, and hydrogen bonding. The schematic highlights how surface protonation at $pH < pH_{pzc}$ enhances uptake of sulfonated anionic dyes through strong Coulombic interactions, whereas deprotonated surfaces at $pH > pH_{pzc}$ favor the adsorption of cationic aromatic dyes via π - π stacking and donor–acceptor interactions. By visualizing these complementary pathways, Figure 2 provides a mechanistic framework explaining how engineered BMO-NCs tailor surface chemistry to achieve high-affinity, dye-specific adsorption under varying wastewater conditions.

Anionic dyes

Congo red (CR) and Eriochrome black T (EBT) are anionic dyes that exhibited a negative charge in solution, owing to the presence of sulfonate groups and other ionizable functional groups in their molecular structures (Al-Zoubi et al.,

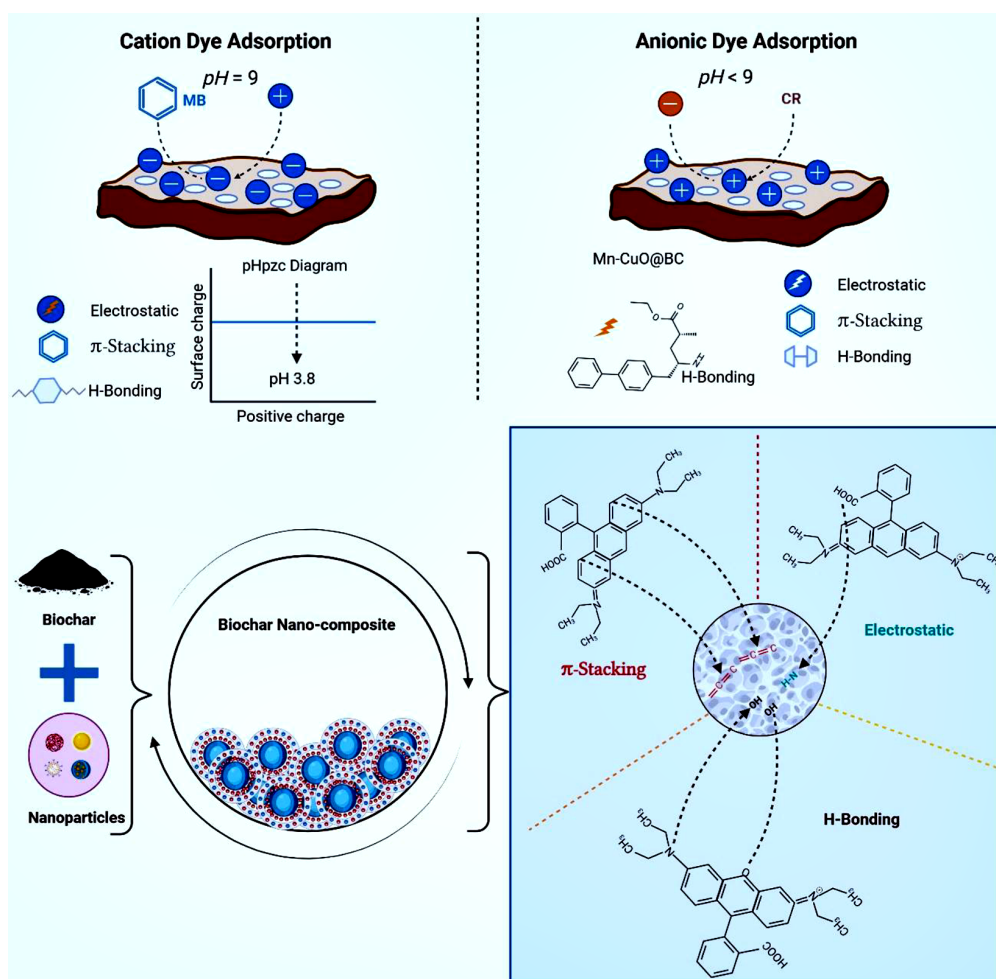


Figure 2. Charge-dependent adsorption mechanisms of cationic and anionic dyes on BMO-NCs, illustrating pH-driven surface charge transitions relative to pHpzc and the dominant interaction pathways electrostatic attraction, π - π stacking, and hydrogen bonding governing dye binding

2020). Effective removal strategies for these dyes often involve the use of positively charged adsorbent surfaces to facilitate electrostatic attraction (Zhang et al., 2019). A positively charged surface can be achieved by adjusting the solution pH to below the material PZC, leading to saturation of positive hydrogen ions on the surface (Al-Amrani et al., 2022). Mn-CuO@BC NCs show that optimal adsorption of anionic dyes like CR and EBT at pH 4, occurred via surface protonation electrostatic attraction. This implies a positively charged surface at low pH, while amine functionalization is discussed in the context of N-doped biochar and as potentially enhancing catalytic activity through improved electron transfer, the provided sources do not explicitly detail amine functionalization or connect it directly as a design strategy for removing anionic dyes like EBT and CR via H^+ saturation at low pH for Mn-CuO@BC NCs. Mn-CuO@BC NCs showed remarkable

adsorption efficiencies of approximately 98% for CR and 95% for EBT. Zeta Potential (ZP) characterization was performed for Mn-CuO@BC to evaluate its stability, and its performance for anionic dyes is better in acidic conditions due to a positively charged surface (Ullah et al., 2025). Similar studies conducted have shown that pH significantly affects the surface charge of adsorbents and their efficiency in removing the Congo Red (CR) dye. The results indicated that pH 2 is the most effective for CR removal, as the adsorbent surfaces acquire a positive charge, promoting electrostatic attraction with the negatively charged dye (Rubangakene et al., 2023).

Azo dyes

The presence of the stable azo bond ($-N=N-$) makes azo dyes a significant environmental hazard (Ramamurthy et al., 2024). Degradation

often involves breaking these bonds, frequently through photocatalysis, which generates reactive oxygen species (ROS) (González and Jaramillo-Fierro, 2025; Qian et al., 2024). Metal oxides embedded into biochar metrics function as catalytic active site, facilitating the production of ROS (Diaz-Urbe et al., 2024). Mn-CuO@BC NCs, containing CuO, were effective in the photocatalytic degradation of azo dyes like CR and EBT. The integration of H₂O₂ with the Mn-CuO@BC system significantly enhanced the photocatalytic degradation of EBT and CR, likely due to the accelerated generation of hydroxyl radical ($\cdot\text{OH}$) (Karuppasamy et al., 2022; Ullah et al., 2025). Moreover, other active substances generated during photocatalysis include $\cdot\text{O}_2^-$ and h^+ . These active species attack and degrade the complex molecular structures of azo dyes into simpler substances (Selvaraj et al., 2021). Analysis of EBT degradation products suggests that the azo -N=N- double bond is a susceptible site for attack by $\cdot\text{OH}$ radicals. Cu/Cu₂O/BC NCs, containing Cu and Cu₂O, generate $\cdot\text{O}_2^-$ and h^+ upon exposure to visible light radiation, the azo dye methyl orange undergoes oxidation and reduction reaction resulting in H₂O and CO₂ (Bekele et al., 2024).

Green synthesis routes

The green synthesis of engineered BMO-NCs is crucial for sustainable textile wastewater

remediation, emphasizing circular resource use, low environmental impact, and industrial feasibility. Biomass precursors, such as agronomic residue, marine biomass, and municipal waste significantly influence the porosity, surface chemistry, and mineral content of the resulting biochar, enabling tailored performance and regional valorization (Khandaker et al., 2025). One-pot synthesis methods (e.g., co-pyrolysis) offer energy efficient, solvent minimized fabrication but often sacrifice precise control over nanoparticle crystallinity and dispersion. In turn, two step approaches (e.g., impregnation calcination) provide tunable surface and structural features at the cost of increased processing complexity (Amrute et al., 2021; Pavlenko et al., 2022; Rao et al., 2024). Key synthesis variables, including temperature, pH, activating agents, and metal doping directly impact BET surface area, pH_{pzc}, zeta potential, magnetic separability and heterojunction formation, which are critical for adsorption and photocatalysis (Amdeha, 2024; Weidner et al., 2022). Scalable methods must also address energy efficiency, compatibility with continuous reactor systems, reusability, and regulatory compliance (e.g., metal leaching, waste generation) (Durak, 2023; Tawo and Mbamalu, 2025). Future advancements should prioritize the synthesis strategies that harmonize environmental safety, material performance, and industrial scalability for real-world deployment. Figure 3 shows the

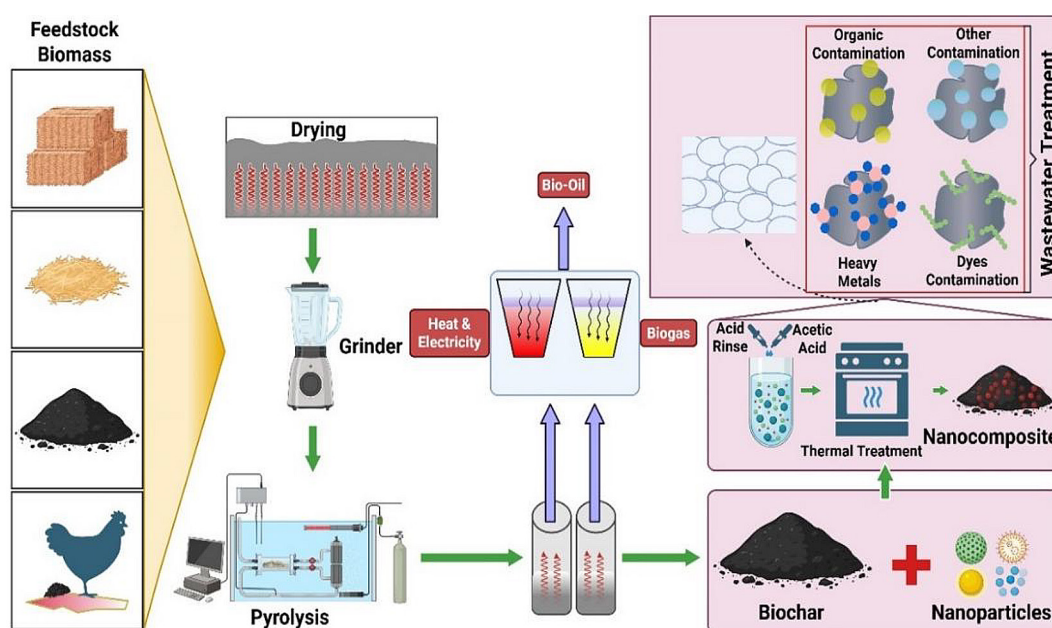


Figure 3. Schematic overview of biochar–metal oxide nanocomposite synthesis from diverse biomass feedstocks through drying, grinding, and pyrolysis, followed by nanoparticle integration and application in wastewater treatment for removing dyes, heavy metals, and organic contaminants

complete synthesis workflow of biochar–metal oxide nanocomposites, beginning with biomass drying, grinding, and pyrolysis to generate a porous carbon framework, followed by metal oxide loading through approaches such as impregnation, hydrothermal treatment, or chemical precipitation. The schematic illustrates how these sequential steps lead to nanoparticle anchoring, surface functionalization, and heterojunction formation, collectively enabling the composite's enhanced adsorption capacity and photocatalytic activity in wastewater treatment.

Comparative analysis of biochar-metal oxide nanocomposites

To rigorously assess the efficiency and scalability of biochar BMO-NCs in dye remediation, a comparative analysis of their physicochemical characteristics, dual-functional performance, and robustness under real effluent conditions is essential. The addition of metal oxides into biochar matrices significantly enhances the surface area, modulates surface charge via pH_{pzc} tuning, and introduces active sites conducive to both adsorption and photocatalysis (Amdeha, 2024; Weidner et al., 2022). Notably, the NCs combining high porosity with appropriate band alignment demonstrate superior dye removal efficiencies (>90%) across varying pH and ionic strength (Zhang et al., 2023). However, performance gaps remain between ideal lab conditions and complex industrial effluents, where co-contaminants, salinity, and fluctuating pH compromise efficacy (Hossain, 2021). Therefore, parameters such as regeneration efficiency, recyclability, and real matrix compatibility are critical for field translation. Table 1 presents a curated comparison of recently developed BMO-NCs, highlighting their compositional features, mechanistic insights, and practical treatment potential.

MECHANISMS OF DYE REMOVAL IN REAL WASTEWATER SYSTEMS

The multifaceted challenges of industrial textile wastewater, characterized by fluctuating pH, high salinity, and co-contaminants, demand more than just high removal efficiencies; they require a fundamental understanding of how engineered BMO-NCs function under harsh, realistic conditions (Dzoujo et al., 2024). While these NCs

leverage a potent synergy of adsorption and photocatalysis for targeted dye removal, their true potential hinges on mechanistic robustness against real-world stressors (Kumar and Singh, 2025). This section dissects the charge transfer pathways, reactive oxygen species (ROS) generation, and interfacial dynamics that govern performance in complex matrices, bridging material design with progress toward clean water and sanitation (Sustainable Development Goal 6).

Synergistic adsorption-photo catalysis in complex matrices

Engineered BMO-NCs typically initiate dye removal through adsorption, an essential pre-concentration step attributed to the essential properties of biochar support (Damahe et al., 2024). Biochar, derived from various biomass sources, possesses various active sites for pollutant capture. The adsorption mechanism involves several mechanisms, such as hydrophobic interactions, pore filling, hydrogen bonding, π - π bonding, and electrostatic interactions between the dye molecules and the biochar surface (Qiu et al., 2022; Tran et al., 2017).

Modifying biochar through metal oxide can further enhance its surface area and introduce new functional groups, thereby increasing its adsorption capacity. Moreover, metal engraving shown to be specifically enhance the biochar surface area, improving its adsorbent properties (Liu and Zhang, 2022). For instance, the ZnO/peanut shell-derived biochar NCs exhibited an 826.44 mg g⁻¹ MB adsorption capacity, significantly improving the recently published adsorbent capacity. Similarly, the adsorption capability of the ZnO/green pea peel biochar (GPBC) NCs amounting to 114.94 mg/g for CR, was particularly higher than for GPBC alone (62.11 mg/g). Modification of date palm-derived biochar with iron (Fe) significantly increased adsorption capacity of MB to 85.21 mg g⁻¹, highlighting the efficiency of the treatment compared to pristine material (Aziz et al., 2024). According to the previous studies, the adsorption follows pseudo-second order kinetics, indicating chemisorption as a predominant mechanism, while adsorption isotherms frequently align with the Langmuir model (Guo et al., 2020). The frequent occurrence of pseudo-second-order kinetics in dye adsorption onto biochar-metal-oxide composites suggests that uptake is influenced by the availability and ionization state of surface

Table 1. Comparative overview of engineered biochar-metal oxide nanocomposites in terms of physicochemical properties, dye removal performance, mechanistic insights, and real wastewater treatment applicability

| Composite | BET (m ² /g) | PZC (pH) | Zeta potential (mV) | Target dye(s) | Adsorption capacity (mg/g) | Removal efficiency (%) | Mechanism (s) | Real wastewater performance | References |
|--------------------------------|-------------------------|----------|-----------------------|-------------------|----------------------------|------------------------|-------------------------------------|-----------------------------|----------------------------|
| ZnO/ peanut shell biochar | 80.6 | 3.8 | -25 (pH 7) | MB | 65.3 | 88–99.81 | Electrostatic | N/A | (Yu et al., 2023) |
| Mn-CuO@ biochar | 3.34 | 5.5/4.0 | +58.8 | CR, EBT | 10.2 | 98 CR, 95 EBT | Chemisorption, Langmuir | Retained over seven cycles | (Ullah et al., 2025) |
| CuO@BSS (barley straw BC) | 80.6 | 3.8 | Negative across pH | MB | 70.4 | 85–99 | Adsorption + Photocatalysis | Tested (efficiency drops) | (Gomaa et al., 2022) |
| PEG-ZnO/rGO | 45 | 3 | | CR | 97.462 | 94 | Adsorption | Real river water tested | (Buledi et al., 2024) |
| MCH-EGDE/ ORNC | | 4.0 | | RBBR | 168.4 | 87.5 | Freundlich, pseudo-2nd-order | N/A | (Abdulhameed et al., 2024) |
| AlS/Pin | | | -20 | MG | 384.61 | 89.98 | Langmuir, pseudo-2nd-order | N/A | (Kolya & Kang, 2025) |
| Chitosan-treated nanocomposite | 8.9 | 7.0 | | MO | 172.17 | 92 | Langmuir | N/A | (Waliullah et al., 2023) |
| Biochar/Ag NPs | 72.6 | 5.2 | -27.5 | MB | 115.2 | 96.09 | Adsorption + Photocatalysis | 84% (textile effluent) | (Chakhtouna et al., 2023) |
| ZnO/GPBC | 112.4 | 7.1 | +15 (pH 4) | CR | 114.94 | 93 | Adsorption | N/A | (Damahe et al., 2024) |
| KOH Lychee seed BC | 154 | 7 | -12.6 | MB | 124.5 | 91 | π - π , H-bonding, Langmuir | N/A | (Rawat et al., 2023) |
| Biochar/Fe oxide (coffee) | | 6.2 | | MB, MO | 62.1 (MB), 57.1 (MO) | 88 | Adsorption > Photocatalysis | N/A | (Kochito et al., 2024) |
| Fe oxide/ Douglas biochar | 91.4 | 5.8 | Positive (protonated) | MB | 210 | 96 | Adsorption | N/A | (Samaraweera et al., 2023) |
| FexOy/date palm BC | | 6.0 | | MB | | 93 | π - π , H-bonding | N/A (4 cycles reusable) | (Abd-Elhamid et al., 2024) |
| AWBM (Wakame BC) | | 5.9 | | MB, hB, MG | 841.6, 33.8, 4066.9 | 95 | Endothermic adsorption | N/A | (Sutar et al., 2022) |
| EPAC (Enteromorpha BC) | | 5.6 | | MB | 910 | 94 | Endothermic, pH-dependent | N/A | (Mittal et al., 2022) |
| Ulva Reticulata BC | | 2.0 | | Remazol Orange 3R | | 91.6 | Bio decolorization | N/A | (Kumar et al., 2021) |

sites, though strictly speaking the model does not prove chemisorption (Devi et al., 2024). Furthermore, many studies report a distinct intraparticle-diffusion regime, particularly for hierarchically porous materials, indicating that external adsorption followed by pore migration contributes to the overall rate (Ahmaruzzaman et al., 2025). Accordingly, kinetic parameters such as the PSO rate constant (k_2) and intraparticle-diffusion coefficient (k_i/d) may reflect, in a semi-quantitative way, how well surface charge, functional groups and pore architecture have been tuned, especially under varied ionic strength or dye-type conditions.

The initial adsorption step concentrates dye molecules on the NCs surface, enhancing proximity to photocatalytic sites and significantly boosting degradation efficiency, even at low pollutant concentrations (Cheng et al., 2022). Engineered NCs like Mn-CuO@BC have shown dual functional advantages, exhibiting remarkable adsorption of 98% for CR and 95% for EBT, which contributes to their high overall removal efficiency. The best adsorption-photocatalytic effect for the Cu/Cu₂O/BC NCs was observed of BC to Cu/Cu₂O (0.2) at specific mass ratio, highlighting the importance of NCs composition for optimal synergistic

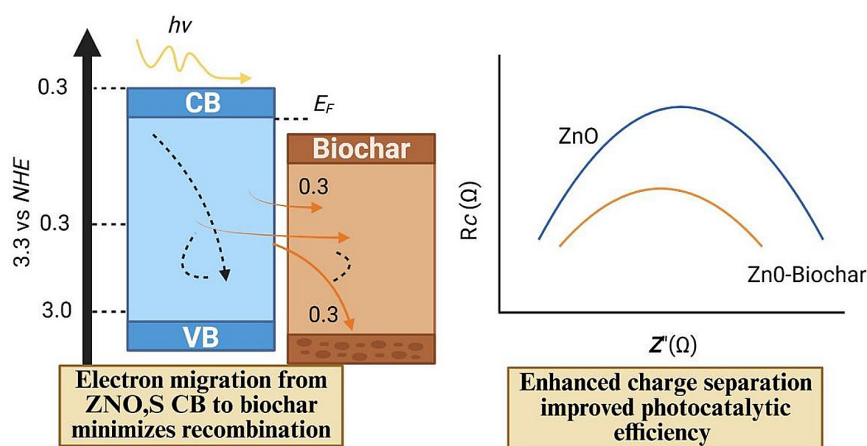


Figure 4. Synergistic adsorption photocatalysis and charge transfer pathways in BMO-NCs enabling enhanced dye degradation under light exposure

performance (Du et al.). Figure 4 shows the charge-transfer behavior of the ZnO–biochar composites, illustrating how photogenerated electrons migrate from the ZnO conduction band to the biochar, reducing electron hole recombination. The left panel depicts band alignment and electron flow under light irradiation, while the right panel shows the reduced charge-transfer resistance (R_{ct}) for the ZnO biochar compared to pure ZnO, confirming enhanced charge separation and improved photocatalytic efficiency.

Charge transfer pathways and ROS generation

Under appropriate light irradiation, the metal oxide component of the BMO-NCs absorbs photons, exciting electrons (e^-) from valance bond (VB) to conduction band (CB) and generating electrons (e^-) in (CB) and holes (h^+) in the VB (Magdalane et al., 2017). A critical aspect of the charge transfer pathway is the efficient separation and transfer process of these photo-generated electron hole pairs, which prevents their rapid recombination and enhances photocatalytic activity (Balapure et al., 2024). The biochar support material perform key role in this by facilitating the migration and transport of these charge carriers due to its electrical conductivity, large surface area, and porosity (Wang et al., 2024). This integration with biochar reduces the probability of electron-hole recombination, making more carriers available for reactions (Liang et al., 2024). Biochar can act as an electron transfer medium, efficiently shuttling photogenerated electrons and channeling them to other components, creating

an extended electron transport path (Javanmard et al., 2024).

Specific charge transfer mechanisms, such as Z-scheme pathways or the transfer of electrons to metal or biochar components in systems like $NiFe_2O_4/ZnIn_2S_4$, further enhance spatial charge separation (Xu et al., 2024). The presence of surface functional groups and defect sites on biochar also promotes rapid electron transfer. This facilitated charge transfer process ultimately drives the generation of reactive oxygen species (ROS) or enables direct redox reactions with adsorbed dye molecules, thereby leading to efficient dye degradation in real wastewater environments (Takhar and Singh, 2025). Experimental evidence from techniques like Electrochemical Impedance Spectroscopy (Mutlu et al.) and photocurrent measurements supports these improved charge transfer dynamics in biochar metal oxide NCs, which shows lower resistance and stronger photocurrents, indicative of faster charge transfer and better carrier separation (Damahe et al., 2024).

The photocatalytic degradation of dyes in engineered BMO-NCs fundamentally relies on ROS generation, yet mechanistic validation remains critically underdeveloped (Damahe et al., 2024). In turn, hydroxyl radicals ($\cdot OH$) and superoxide anions ($\cdot O_2^-$) are frequently considered as primary reactive species. Figure 5 shows the combined adsorption–photocatalytic pathway of ZnO–biochar nanocomposites. Cationic and anionic dyes are first adsorbed onto the biochar surface through electrostatic interactions, while ZnO activates under light to generate reactive oxygen species ($\cdot OH$, $\cdot O_2^-$). Previous studies highlighted that, electron spin resonance (ESR) spectroscopy

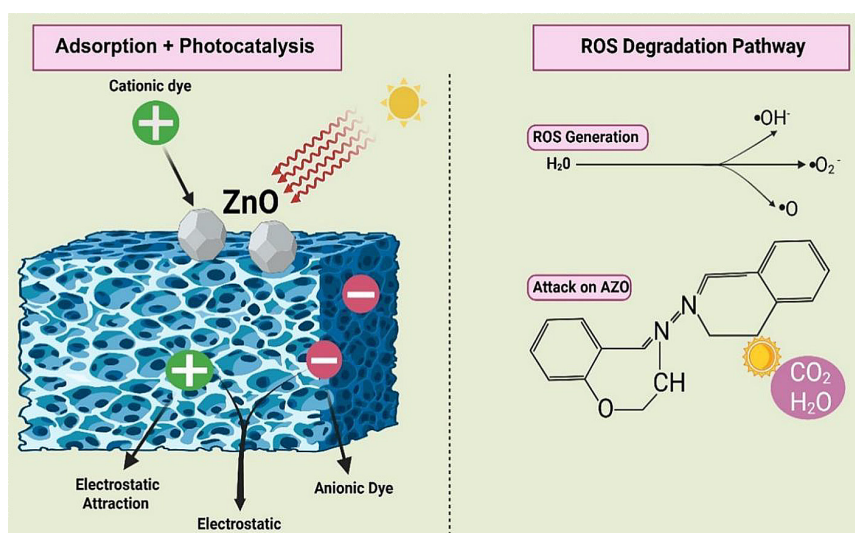


Figure 5. Integrated adsorption–photocatalytic dye removal on metal oxide biochar composites, showing electrostatic adsorption of cationic and anionic dyes followed by ROS-mediated azo-bond cleavage and mineralization into CO_2 and H_2O

with spin-trapping agents (e.g., DMPO) can be used to detect diagnostic signatures of $\text{DMPO}\cdot\text{OH}$ (1:2:2:1 quartet) or $\text{DMPO}\cdot\text{O}_2$ adducts (Jiang et al., 2021). In their absence, mechanistic claims rest on circumstantial correlations rather than spectroscopic proof. Quantitative ROS metrics are often missing, especially in the H_2O_2 -assisted systems where gains are vaguely linked to increased $\cdot\text{OH}$ without mechanistic insight (Brandes et al., 2018). The sustained generation of reactive oxygen species (ROS) in BMO-NCs is critically dependent on the efficient redox cycling of the incorporated metal centers (e.g., $\text{Fe}^{2+}/\text{Fe}^{3+}$, $\text{Cu}^+/\text{Cu}^{2+}$, $\text{Mn}^{3+}/\text{Mn}^{4+}$). This cycling acts as a catalytic engine for ROS regeneration. For instance, in a Fenton-like system, a surface-bound Fe^{2+} site activates H_2O_2 to yield a hydroxyl radical ($\cdot\text{OH}$) and Fe^{3+} ($\text{Fe}^{2+} + \text{H}_2\text{O}_2 \rightarrow \text{Fe}^{3+} + \cdot\text{OH} + \text{OH}^-$) (Zhang et al., 2024). The photocatalytic role of the composite is crucial here: photogenerated electrons from the metal oxide or conductive biochar matrix subsequently reduce Fe^{3+} back to Fe^{2+} ($\text{Fe}^{3+} + \text{e}^- \rightarrow \text{Fe}^{2+}$), closing the loop and allowing the catalytic consumption of H_2O_2 to continue (Xue et al., 2025). Similarly, $\text{Cu}^+/\text{Cu}^{2+}$ pairs facilitate the $\cdot\text{OH}$ production from H_2O_2 or peroxy-monosulfate (PMS), while their interconversion is driven by electron transfer processes that prevent the active sites from being passivated in a higher oxidation state. This continuous electron shuttling is fundamental to maintaining a high flux of radicals for the degradation of pre-concentrated

dye molecules (Feng et al., 2024; Wang et al., 2024). In reality, H_2O_2 amplifies ROS through three distinct pathways: (i) as an electron acceptor facilitating O_2 reduction to $\cdot\text{O}_2^-$ ($\text{O}_2 + \text{e}^- \rightarrow \cdot\text{O}_2^-$); (Rubangakene et al.) via Fenton-like reactions at metal sites ($\text{M}^{n+} + \text{H}_2\text{O}_2 \rightarrow \text{M}^{(n+1)+} + \cdot\text{OH} + \text{OH}^-$); and (iii) through Haber cycles, where $\cdot\text{O}_2^-$ disproportionate H_2O_2 ($\cdot\text{O}_2^- + \text{H}_2\text{O}_2 \rightarrow \cdot\text{OH} + \text{OH}^- + \text{O}_2$) (Rangarajan et al., 2022). Kinetic validation of these pathways is rare, and literature employs radical scavengers (isopropanol for $\cdot\text{OH}$, p-benzoquinone for $\cdot\text{O}_2^-$, EDTA for h^+) to deconvolute their contributions.

In addition to well-known reactive species such as $\cdot\text{OH}/\cdot\text{OH}/\cdot\text{OH}/\cdot\text{OH}/\cdot\text{O}_2^-$, other high-potential oxidants are systematically overlooked. Photogenerated h^+ directly oxidizes dyes via surface bound reactions ($\text{dye} + \text{h}^+ \rightarrow \text{dye}^+\cdot \rightarrow \text{fragmentation}$), while singlet oxygen ($^1\text{O}_2$), generated through energy transfer to dissolved O_2 , cleaves electron-rich azo bonds ($-\text{N}=\text{N}-$) (Li et al., 2024). Despite the established detection methods, these reactive species are rarely characterized experimentally, notably using furfuryl alcohol as a selective $^1\text{O}_2$ probe ($k = 1.2 \times 10^8 \text{ M}^{-1}\cdot\text{s}^{-1}$) or ammonium oxalate for hole (h^+) scavenging (Shawky et al., 2024). In persulfate activated systems ($\text{S}_2\text{O}_8^{2-}/\text{HSO}_5^-$), sulfate radicals ($\text{SO}_4\cdot^-$, $E^\circ = 2.5\text{--}3.1 \text{ V}$) likely dominate degradation due to superior selectivity toward conjugated systems, yet their role in biochar metal oxide NCs remains uninvestigated (Sutar et al., 2022).

Mechanistic validation: ROS quantification and degradation pathways

Connecting lab research to industry requires thorough mechanistic validation. While various studies highlight the role of reactive oxygen species (ROS), such as $\cdot\text{OH}$ and $\cdot\text{O}_2^-$ in dye degradation, experimental evidence is scarce. Electron spin resonance (ESR) and in situ spectroscopy should help understand reactive species. Liquid chromatography mass spectrometry (LC-MS) can also track dye breakdown paths, identify intermediates, and verify that the degradation process is complete and safe. Degradation pathway mapping suffers from inadequate resolution (Xie et al., 2022). While azo bond cleavage is universally acknowledged, intermediate speciation is rarely tracked (Mutlu et al., 2018). Liquid chromatography mass spectrometry (LC-MS) could reveal sequential transformations: initial (-N=N-) scission generating anilines/naphthylamines, followed by aromatic ring hydroxylation, desulfonation (-SO₃H loss), and ultimate mineralization to aliphatic acids (e.g., oxalate, formate). In the absence of comprehensive carbon tracking, claims of complete mineralization based solely on chemical oxygen demand (COD) reduction remain problematic, since COD quantifies oxidizable species, rather than verifies complete carbon conversion to CO₂ (Oliveira et al., 2023). Total organic carbon (TOC) analyses reported in a study reveal significant shortfalls. Toxicity assessments (e.g., ECOSAR) without structural confirmation of intermediates risk underestimating ecological hazards from residual by-products (Shi et al., 2023).

Biochar itself may act as a ROS sink, its graphitic domains and redox active quinones competitively consume radicals. Consequently, ROS fluxes measured in synthetic dye solutions overestimate real-system performance by 2–5 fold (Xie et al., 2024). Bridging this lab-field divide demands ESR validation of ROS identities/yields, scavenger studies to quantify pathway contributions, LC-MS elucidation of degradation cascades, and TOC based mineralization tracking in complex effluents. Only through such mechanistic rigor can NCs progress from promising concepts to deployable technologies.

Performance challenges in industrial effluents

Industrial effluents contain complex matrices comprising mixed dyes, co-contaminants (including heavy metals and ionic species), and dynamic

physicochemical conditions (pH fluctuations, variable salinity), all of which critically influence nanocomposite performance and treatment efficacy (Omorieg et al., 2023). The presence of other organic and inorganic species, including ionic species, can compete with targeted pollutants for active adsorption sites, thereby reducing adsorption capacities (Zhao et al., 2021). Increasing ionic strength, for instance, has been observed to decrease the adsorption of pollutants (Zhang et al., 2019). The wastewater from industries like textiles is particularly complex, containing a diverse array of hazardous organic and inorganic chemicals, often at high temperatures with varying pH, high conductivity, and significant organic matter. Addressing multiple dyes and competing pollutants is key to improving reliability and scalability. Most studies, however, still rely on synthetic dye solutions under ideal laboratory conditions, which limits validation in real industrial effluents (Catarino et al., 2025; Tsauria et al., 2025; Yaseen and Scholz, 2019).

Despite these challenges, some materials have demonstrated potential when tested in complex matrices or real water samples. For instance, Mn-CuO@BC NCs retained approximately 75% CR removal efficiency in textile wastewater, despite competing organics, highlighting their resilience in complex matrices. CuO@BSS, when evaluated using real water samples (agricultural water, Nile River water, and industrial wastewater), achieved high MB removal efficiencies, including 99% photodegradation for 10 mg/L MB in agricultural water (Gomaa et al., 2022). The reduced MB removal efficiency observed in these real samples was attributed to the competition from other co-existing organic and inorganic species for surface active sites. Moreover, ZnO/peanut shell biochar removed more than 50% of chemical oxygen demand (COD) and 82.2% turbidity from real textile wastewater, significantly improving water quality and support achievement SDG 6 targets (Attiqa Ahmad et al., 2024).

Mineralization, indicated by total organic carbon (TOC)/COD decline, is a crucial metric beyond simple color removal (Kovo et al., 2023). Despite the successes in color and turbidity removal, significant gaps persist in thoroughly evaluating material performance under realistic conditions. Real industrial wastewater, with its complex mixtures, fluctuating pH, high salinity, and competing co-contaminants, can drastically reduce efficacy compared to laboratory tests

(Sibhatu et al., 2022). Future research must therefore prioritize testing adsorbents under diverse and dynamic conditions on real industrial wastewater to ensure efficacy, exploring competitive adsorption in actual complex pollutant systems (Selim et al., 2024). While some materials show insensitivity to pH fluctuations, further investigation into the impact of ionic strength and competing pollutants is necessary (Zhang et al., 2019).

Biochar-metal oxide and polymer nanocomposites for dye remediation

BMOs-NCs utilize waste biomass such as agricultural residues or municipal waste, enabling cost-effective synthesis aligned with circular economy principles (Akhtar et al., 2024). These materials demonstrate superior adsorption capacities for diverse dyes while enhancing sustainability through resource valorization. Conversely, PNCs leverage tunable synthetic matrices like PMMA/OMMT or cellulose/polyaniline, offering advantages in cost efficiency and process scalability (Antony Jose et al., 2025). However, PNCs raise environmental concerns due to fossil-derived monomers (Ciardelli et al., 2019). Both material classes show promising reusability across multiple regeneration cycles, yet scalability remains constrained by minimal industrial pilot validation (Singh et al., 2025). Critical research gaps persist in three areas: rigorous economic assessments of synthesis costs, comprehensive lifecycle evaluations of environmental footprints, and compliance validation against international regulatory standards (Pucciarelli, 2023). Industrial metrics, like reactor throughput and energy consumption remain severely underreported in real effluents. Neither technology currently employs AI/ML for design optimization nor adapts to regional variables, such as biomass availability. To advance these materials beyond lab-scale promise, future work must prioritize standardized economic benchmarks, industrial pilot demonstrations in complex wastewater, and regulatory integration frameworks (Akhrame et al., 2018; Kumar et al., 2024).

DISCUSSION

Addressing the persistent challenge of dye-contaminated wastewater treatment necessitates a clear vision toward future advancements, overcoming existing barriers, and ensuring practical,

safe, and policy-aligned implementation of novel technologies such as PNCs and metal oxide-biochar nanoparticles.

Limitations of current research

A primary limitation in current research is the predominant use of synthetic dye solutions in laboratory settings, which often fails to capture the complexity of real industrial effluents containing intricate dye mixtures, fluctuating pH levels, and various co-existing contaminants (Amdeha, 2024). While materials like gelatin NCs have demonstrated high adsorption capacities (e.g., 950.5 mg/g), their efficacy in realistic wastewater scenarios remains largely unproven (Elella et al., 2022).

Technical challenges in material synthesis and performance

Key challenges requiring technical solutions include issues inherent in material synthesis and performance. Batch variability is a notable concern, particularly for biochar production, where the heterogeneous nature of biochar feedstocks or varying preparation conditions can yield materials with inconsistent properties. While green synthesis routes using plant extracts are promising from an eco-friendly perspective, they may contribute to this variability, making standardized production difficult (El-Hussein et al., 2024; Hano and Abbasi, 2022). Another critical challenge, especially concerning MBOs-NCs, is the potential for metal leaching from the nanoparticles into the treated water or environment (Dey and Ahmaruz-zaman, 2023). Although the sources highlight the toxicity of heavy metals found in some dyes and the need to minimize secondary pollution from catalyst precursors, they do not explicitly detail silica encapsulation as a mitigation strategy; however, the general need to assess and mitigate environmental risks and toxicity is recognized. Beyond synthesis, performance challenges include the decrease in removal efficiency after multiple reuse cycles due to the blockage of active sites on the adsorbent surface, necessitating enhanced surface modifications for improved regeneration capabilities (Abdullah et al., 2025; Tripathy et al., 2024). The toxic phenomenon of nanoparticle re-agglomeration in NC materials, driven by strong Van der Waals interactions and, electrostatic also poses a challenge, which might be addressed by creating long-chain carbon materials in the structure of NCs (Jose et al., 2025).

Future opportunities for advanced materials

Future research must decisively shift focus from single synthetic dyes to the treatment of complex dye cocktails and real industrial wastewater under diverse and dynamic conditions to ensure reliability and scalability. This necessitates the development of tailored materials, engineered explicitly for selectivity and efficiency in treating such intricate pollutant mixtures, potentially also targeting the degradation of multiple pollutants simultaneously. Furthermore, comprehensive cost analyses, encompassing material synthesis, regeneration potential, long term feasibility, and lifecycle impact assessments, are important for evaluating the economic feasibility of these technologies. The reusability of materials is vital for cost-effectiveness in large-scale applications.

Policy and regulatory frameworks for sustainable implementation

The successful adoption and impact of these wastewater treatment technologies are inextricably linked to supporting policy and regulatory frameworks. Literature does not specifically detail incentives like eco certification or tax credits; they strongly advocate for developing sustainable, eco-friendly, and cost-effective solutions for dye removal. Promoting closed-loop textile processing, where treated water is potentially reused, aligns with the broader goals of environmental protection and resource conservation. Aligning these research and development efforts with international initiatives like the United Nations Sustainable Development Goal 6 (SDG 6) concerning clean water and sanitation, and the principles of the EU Circular Economy Action Plan.

Finally, there is a pressing need for standardization within the field. This includes developing standardized synthesis protocols and comprehensive characterization techniques for novel materials. The establishment of standardized protocols for dye testing in real wastewater, potentially through international bodies like ISO or ASTM, is critical to ensure data reproducibility, comparability, and reliable evaluation of different treatment technologies across various studies and applications. By addressing these challenges and embracing future opportunities, the research community can contribute significantly to the development and deployment of effective, scalable, and ecological solutions for industrialized dyes discharge treatment, safeguarding water resources and environmental health.

CONCLUSIONS

Biochar metal oxide nanocomposites (BMO-NCs) represent a highly promising class of dual-functional materials capable of delivering sustainable and efficient treatment of textile wastewater. Their synergistic combination of high-surface-area adsorption and photocatalytic degradation enables the removal of complex dye structures while minimizing chemical inputs and energy consumption. However, the substantial performance gap between laboratory conditions and real industrial effluents characterized by variable pH, high salinity, and competing contaminants underscores the need for more rigorous mechanistic understanding and realistic evaluation frameworks. Advancing this field will require in-situ ESR verification of reactive oxygen species, LC-MS tracking of degradation intermediates, long-term regeneration and leaching studies, and standardized testing protocols tailored for complex waste streams. Equally important is the development of scalable, low-energy synthesis routes and the integration of BMO-NCs into pilot and continuous-flow treatment systems. With these scientific and engineering advancements, BMO-NCs have the potential to mature into robust, ecologically safe, and scalable technologies, offering a transformative pathway toward sustainable wastewater management and meaningful progress toward Sustainable Development Goal 6.

Acknowledgments

This study was supported by the National Natural Science Foundation of China (Grant No. 42177431), the Beijing Natural Science Foundation (International Scientists Project, Grant No. IS25086), and the Inner Mongolia Department of Science and Technology Project (Grant No. 2024ZY0096). The team appreciate for the support from China Scholarship Council and TYSP program to the international students and scholars.

REFERENCES

1. Abd-Elhamid, A.I., Nayl, A.A., Akl, M.A., Mosnáčková, K., and Aly, H.F. (2024). *Application of Engineered Biochar for Wastewater Treatment*. In: *Catalytic Applications of Biochar for Environmental Remediation: A Green Approach Towards Environment Restoration*. ACS Publications, 11, 223–246.

2. Abdulhameed, A.S., Hapiz, A., Musa, S.A., AlOthman, Z.A., Wilson, L.D., and Jawad, A.H. (2024). Biomagnetic chitosan-ethylene glycol diglycidyl ether/organo-nanoclay nanocomposite for azo dye removal: A statistical modeling by response surface methodology. *International Journal of Biological Macromolecules*, 255, 128075.
3. Abdullah, A., Zumra, Z., and Ahmed, S. (2025). Recent innovations in nanocomposite beads for the removal of pollutants from water: a critical review. *Environmental Science: Water Research and Technology*, 11, 1428–1445.
4. Adawiyah, R., Yuliasari, N., Hanifah, Y., and Palapa, N. R. (2025). Areca Catechu biochar and nanobiochar as adsorbents for Congo Red: Synthesis, characterization, and performance evaluation. *Bulletin of Chemical Reaction Engineering and Catalysis*, 0(1), 112–128.
5. Ahmad, A., e Noor, A., Anwar, A., Majeed, S., Khan, S., Nisa, Z. U., Ali, S., Gnanasekaran, L., Rajendran, S., and Li, H. (2024). Support based metal incorporated layered nanomaterials for photocatalytic degradation of organic pollutants. *Environmental Research*, 260, 119481.
6. Ahmad, A., Khan, Z.U.H., Sabahat, S., Sun, J., Shah, N.S., Khan, Z.U., Muhammad, N., Mir, S., Rahim, A., and Nadeem, M. (2024). Innovations in metal oxides-biochar nanoparticles for dye removal. *Nano-Structures and Nano-Objects*, 39, 101269.
7. Ahmaruzzaman, M., Roy, S., Singha, A., Rtimi, S., and Aminabhavi, T.M. (2025). Emerging nanotechnologies in adsorption of dyes: a comprehensive review of carbon and metal oxide-based nanomaterials. *Adsorption*, 31(2), 34.
8. Ahmed, M.A., Farag, M., Ahmed, M., Mahmoud, S.A., and Mohamed, A.A. (2025). Enhancing the adsorption capacity of SnS₂-g-C₃N₄ through chitosan integration: Insights from structural and optical characterization. *Surfaces and Interfaces*, 64, 106321.
9. Akhrame, M.O., Fatoki, O.S., Opeolu, B.O., Olorunfemi, D.I., and Oputu, O.U. (2018). Polymeric nanocomposites (PNCs) for wastewater remediation: an overview. *Polymer-Plastics Technology and Engineering*, 57(17), 1801–1827.
10. Akhtar, M. S., Ali, S., and Zaman, W. (2024). Innovative adsorbents for pollutant removal: exploring the latest research and applications. *Molecules*, 29(18), 4317.
11. Akinnike, A., Agboola, O., Edith, A., and Ezinne, I. (2024). The role of catalyst in the adsorption of dye: Homogeneous catalyst, heterogeneous catalyst, and advanced catalytic activated carbon, critical review. *Desalination and Water Treatment*, 320, 100780.
12. Al-Amrani, W.A., Hanafiah, M.A.K.M., and Mohammed, A.-H.A. (2022). A comprehensive review of anionic azo dyes adsorption on surface-functionalised silicas. *Environmental Science and Pollution Research*, 29(51), 76565–76610.
13. Al-Zoubi, H., Zubair, M., Manzar, M.S., Manda, A.A., Blaisi, N.I., Qureshi, A., and Matani, A. (2020). Comparative adsorption of anionic dyes (eriochrome black t and Congo red) onto jojoba residues: isotherm, kinetics and thermodynamic studies. *Arabian Journal for Science and Engineering*, 45, 7275–7287.
14. Altintas Yildirim, O., Bahadir, A.M., and Pehlivan, E. (2024). *The Role and Significance of Biochars for the Photodegradation of Selected Organic Dyes in Water and Wastewater*, Pollutants and Recent Trends in Wastewater Treatment, Springer, Berlin.
15. Amdeha, E. (2024). Biochar-based nanocomposites for industrial wastewater treatment via adsorption and photocatalytic degradation and the parameters affecting these processes. *Biomass Conversion and Biorefinery*, 14(19), 23293–23318.
16. Ameen, A.J.M., Omer, K.M., and Qasim, A.K. (2025). Enhanced adsorption of an organic dye by phyto-synthesized CuO nanoparticles derived from Malva sylvestris for sustainable environmental remediation. *Materials Advances*, 6, 8139–8156.
17. Amrute, A.P., De Bellis, J., Felderhoff, M., and Schüth, F. (2021). Mechanochemical synthesis of catalytic materials. *Chemistry—A European Journal*, 27(23), 6819–6847.
18. Antony Jose, S., Cowan, N., Davidson, M., Godina, G., Smith, I., Xin, J., and Menezes, P. L. (2025). A comprehensive review on cellulose Nanofibers, nanomaterials, and composites: Manufacturing, properties, and applications. *Nanomaterials*, 15(5), 356.
19. Ashebir, H., Tibebe, S., Bedada, D., Fito, J., Kassahun, E., and Worku, A. (2024). Advanced methylene blue adsorption with a tailored biochar/graphene oxide/magnetite nanocomposite: characterization, optimization, and reusability. *Biomass Conversion and Biorefinery*, 15 15885–15906.
20. Aslam, A., Batool, F., Noreen, S., Abdelrahman, E.A., Mustaqeem, M., Albalawi, B.F. A., and Ditta, A. (2024). Metal oxide-impregnated biochar for azo dye remediation as revealed through kinetics, thermodynamics, and response surface methodology. *ACS omega*, 9(4), 4300–4316.
21. Balapure, A., Dutta, J.R., and Ganesan, R. (2024). Recent advances in semiconductor heterojunctions: a detailed review of the fundamentals of photocatalysis, charge transfer mechanism and materials. *RSC Applied Interfaces*, 1(1), 43–69.
22. Bekele, T., Mebratie, G., Girma, A., and Alamnie, G. (2024). Characterization and fabrication of p-Cu₂O/n-CeO₂ nanocomposite for the application of photocatalysis. *Colloids and Surfaces A: Physicochemical and Engineering Aspects*, 685, 133271.

23. Borthakur, P., Aryafard, M., Zara, Z., David, Ř., Minofar, B., Das, M.R., and Vithanage, M. (2021). Computational and experimental assessment of pH and specific ions on the solute solvent interactions of clay-biochar composites towards tetracycline adsorption: Implications on wastewater treatment. *Journal of Environmental Management*, 283, 111989.
24. Brandes, R.P., Rezende, F., and Schröder, K. (2018). Redox regulation beyond ROS: why ROS should not be measured as often. *Circulation research*, 123(3), 326–328.
25. Buledi, J.A., Solangi, A.R., Mallah, A., Batool, M., Shah, Z.-U.-H., and Sherazi, S.T. (2024). Controlled removal of textile azo dye Congo red from aqueous system using PEG-ZnO/rGO composite. *Chemical Papers*, 78(11), 6531–6543.
26. Catarino, M.L., Sampaio, F., and Gonçalves, A.L. (2025). Sustainable Wet processing technologies for the textile industry: A comprehensive review. *Sustainability*, 17(7), 3041.
27. Chakhtouna, H., Ouhssain, A., Kadmiri, I.M., Benzaid, H., Zari, N., el kacem Quaiss, A., and Bouhfid, R. (2023). Photocatalytic and bactericidal behaviors of Ag/TiO₂ doped biochar through Ball-milling approach. *Journal of Photochemistry and Photobiology A: Chemistry*, 444, 114971.
28. Cheng, S., Zhao, S., Xing, B., Liu, Y., Zhang, C., and Xia, H. (2022). Preparation of magnetic adsorbent-photocatalyst composites for dye removal by synergistic effect of adsorption and photocatalysis. *Journal of Cleaner Production*, 348, 131301.
29. Ciardelli, F., Bertoldo, M., Bronco, S., and Passaglia, E. (2019). *Polymers from Fossil and Renewable Resources*. Springer.
30. Damahe, D., Mayilswamy, N., and Kandasubramanian, B. (2024). Biochar/metal nanoparticles-based composites for Dye remediation: A review. *Hybrid Advances*, 6, 100254.
31. Devi, Y. H., Pal, S., Singh, H. H., Singh, M., Singh, N. S., and Singh, L. H. (2024). Surface charge alteration of charcoal derived from bamboo leaves and understanding the interaction with anionic and cationic dye. *Physica Scripta*, 99(10), 1059c1054.
32. Dey, A. K., and Ahmaruzzaman, M. (2023). Recent advances in nano-metal oxide-biochar composites for efficient removal of environmental contaminants. *Reviews of Environmental Contamination and Toxicology*, 261(1), 6.
33. Diaz-Uribe, C., Florez, J., Vallejo, W., Duran, F., Puello, E., Roa, V., Schott, E., and Zarate, X. (2024). Removal and photocatalytic degradation of methylene blue on ZrO₂ thin films modified with Anderson-Polioxometalates (Cr³⁺, Co³⁺, Cu²⁺): An experimental and theoretical study. *Journal of Photochemistry and Photobiology A: Chemistry*, 454, 115689.
34. Du, G., Ding, Y., Li, C., Li, J., Li, M., and Zhu, W. Preparation of Cu/Cu₂O/Bc and its performance in adsorption-photocatalytic degradation of methyl orange in wastewater. *Materials*, 17(17), 4306.
35. Durak, H. (2023). Comprehensive assessment of thermochemical processes for sustainable waste management and resource recovery. *Processes*, 11(7), 2092.
36. Dzoujo, H.T., Shikuku, V.O., Tome, S., Simo, A.C.N., Ng'eno, E.C., Getenga, Z.M., Etoh, M.A., and Dina, D.D.J. (2024). Recent advances in metal oxide-biochar composites for water and soil remediation: a review. *Hybrid Advances*, 7, 100292.
37. Ederer, J., Henych, J., Neubertová, V., Ryšánek, P., Kolská, Z., and Janoš, P. (2025). Influence of substituent position and pH on organophosphates hydrolysis catalyzed by various nanocrystalline ceria. *Journal of Environmental Chemical Engineering*, 13(3), 116460.
38. El-Hussein, A., Mounir, M., El-Sayed, M.A., and Abd El-sadek, M. (2024). Green synthesis of nano materials and their applications, *Comprehensive Analytical Chemistry* 105, 461–491.
39. Elella, M.H.A., Goda, E.S., Gab-Allah, M.A., Hong, S.E., Lijalem, Y.G., and Yoon, K.R. (2022). *Biodegradable polymeric nanocomposites for wastewater treatment, Advances in nanocomposite materials for environmental and energy harvesting applications*, Springer, Berlin.
40. Feng, C., Zhang, H., Guo, J., Yu, S.-Y., Luo, M., Zhang, J., Ren, Y., Liu, Y., Zhou, P., and He, C.-S. (2024). Boosted H₂O₂ utilization and selective hydroxyl radical generation for water decontamination: Synergistic roles of dual active sites in H₂O₂ activation. *Water Research*, 267, 122453.
41. George, G., Ealias, A.M., and Saravanakumar, M. P. (2024). Advancements in textile dye removal: a critical review of layered double hydroxides and clay minerals as efficient adsorbents. *Environmental Science and Pollution Research*, 31(9), 12748–12779.
42. Gomaa, H., Hussein, M.A., Motawea, M.M., Abo-raia, A.M., Cheira, M.F., Alotaibi, M.T., El-Bahy, S.M., and Ali, H.M. (2022). A hybrid mesoporous CuO@ barley straw-derived SiO₂ nanocomposite for adsorption and photocatalytic degradation of methylene blue from real wastewater. *Colloids and Surfaces A: Physicochemical and Engineering Aspects*, 644, 128811.
43. González, S., and Jaramillo-Fierro, X. (2025). Density functional theory study of methylene blue demethylation as a key step in degradation mediated by reactive oxygen species. *International Journal of Molecular Sciences*, 26(4), 1756.
44. Grabi, H., Ouakouak, A., Kadouche, S., Lemlikchi, W., Derridj, F., and Din, A.T.M. (2022). Mechanism and adsorptive performance of ash tree seeds as a

- novel biosorbent for the elimination of methylene blue dye from water media. *Surfaces and Interfaces*, 30, 101947.
45. Guo, S., Zou, Z., Chen, Y., Long, X., Liu, M., Li, X., Tan, J., and Chen, R. (2023). Synergistic effect of hydrogen bonding and π - π interaction for enhanced adsorption of rhodamine B from water using corn straw biochar. *Environmental Pollution*, 320, 121060.
 46. Guo, X., Liu, A., Lu, J., Niu, X., Jiang, M., Ma, Y., Liu, X., and Li, M. (2020). Adsorption mechanism of hexavalent chromium on biochar: kinetic, thermodynamic, and characterization studies. *ACS omega*, 5(42), 27323–27331.
 47. Hailili, R., and Gan, Y. (2025). Tailoring multiscale interfaces in heterojunction photocatalysis for NO_x removal. *ACS Applied Materials and Interfaces*, 17, 39809–39844.
 48. Hakami, O. (2023). Biochar-derived activated carbons: A comprehensive assessment of kinetic and isotherm modeling for adsorptive removal of methylene blue dye contaminants. *International Journal of Environmental Science and Technology*, 20(9), 10325–10344.
 49. Haleem, A., Shafiq, A., Chen, S.-Q., and Nazar, M. (2023). A comprehensive review on adsorption, photocatalytic and chemical degradation of dyes and nitro-compounds over different kinds of porous and composite materials. *Molecules*, 28(3), 1081.
 50. Hama Aziz, K.H., Fatah, N.M., and Muhammad, K.T. (2024). Advancements in application of modified biochar as a green and low-cost adsorbent for wastewater remediation from organic dyes. *Royal Society Open Science*, 11(5), 232033.
 51. Hano, C., and Abbasi, B. H. (2022). Plant-based green synthesis of nanoparticles: Production, characterization and applications. *Biomolecules*, 12(1), 31.
 52. Hossain, M.F. (2021). *Wastewater, Global Sustainability in Energy, Building, Infrastructure, Transportation, and Water Technology*, Springer, Berlin.
 53. Iqbal, A., Yusaf, A., Usman, M., Hussain Bokhari, T., and Mansha, A. (2024). Insight into the degradation of different classes of dyes by advanced oxidation processes; a detailed review. *International Journal of Environmental Analytical Chemistry*, 104(17), 5503–5537.
 54. Javanmard, A., Daud, W. M. A. B. W., Patah, M. F. A., Zuki, F. M., and Verdugo, A. S. (2024). Harnessing the potential of biochar-based catalysts for sustainable adsorptive and photocatalytic applications: a comprehensive review. *Process Safety and Environmental Protection*, 189, 387–413.
 55. Jiang, X., Boudreau, M.D., Fu, P.P., and Yin, J.-J. (2021). Applications of electron spin resonance spectroscopy in photoinduced nanomaterial charge separation and reactive oxygen species generation. *Journal of Environmental Science and Health, Part C*, 39(4), 435–459.
 56. Kar, S., Dey, S., Ghosh, S.K., Ray, N., Mukhopadhyay, J., Kumar, S., Ghosh, S., and Majumdar, S. (2025). Upcycling of polyester based textile fabric waste into surface modified biochar: Assessment of triclosan adsorption efficiency and utilization of used biochar as electrode in supercapacitor. *Materials Chemistry and Physics*, 345, 131207.
 57. Karuppasamy, P., Senthilkumar, S., Ganeshbabu, O., Pitchaimuthu, S., Sennappan, M., and Rajapandian, V. (2022). Sonochemical synthesis and characterization of visible light driven CuO@ g-C₃N₄ nano-photocatalyst for eriochrome black T dye degradation in industrial dye effluent. *Russian Journal of Inorganic Chemistry*, 67(13), 2153–2165.
 58. Kaur, H. (2022). Synergistic effect of biochar impregnated with ZnO nano-flowers for effective removal of organic pollutants from wastewater. *Applied Surface Science Advances*, 12, 100339.
 59. Khandaker, T., Islam, T., Nandi, A., Anik, M.A.-A.M., Hossain, M.S., Hasan, M.K., and Hossain, M. S. (2025). Biomass-derived carbon materials for sustainable energy applications: a comprehensive review. *Sustainable Energy and Fuels*, 9, 693–723.
 60. Kochito, J., Gure, A., Beyene, T.T., and Femi, O.E. (2024). Magnetic iron-oxide coffee husk and khat waste biochar nanocomposites for removal of methylene blue from aqueous solution. *Separation Science Plus*, 7(6), 2300246.
 61. Kolya, H., and Kang, C.-W. (2025). Recent advances in polymer nanocomposites for the adsorptive removal of toxic azo dyes from water. *Discover Water*, 5(1), 28.
 62. Kovo, A.S., Alaya-Ibrahim, S., Abdulkareem, A.S., Adeniyi, O.D., Egbosiuba, T.C., Tijani, J.O., Saheed, M., Okafor, B.O., and Yusuff, A.S. (2023). Column adsorption of biological oxygen demand, chemical oxygen demand and total organic carbon from wastewater by magnetite nanoparticles-zeolite A composite. *Heliyon*, 9(2), a13095.
 63. Kumar, A., Tyagi, P.K., Tyagi, S. et al. (2024). Integrating green nanotechnology with sustainable development goals: a pathway to sustainable innovation. *Discov Sustain* 5, 364.
 64. Kumar, A., Singh, E., and Lo, S.-L. (2025). Tunable 2D porous Ti₃C₂T_x MXene@ biochar composites synthesized via ultrasound-assisted self-assembly for simultaneous removal of co-existing wastewater contaminants. *Separation and Purification Technology*, 355, 129648.
 65. Kumar, M., Gokulan, R., Sujatha, S., Shanmuga Priya, S.P., Praveen, S., and Elayaraja, S. (2021). Biodecolorization of Reactive Red 120 in batch and packed bed column using biochar derived from *Ulva reticulata*. *Biomass Conversion and Biorefinery*, 13, 1707–1721.

66. Kumar, P., and Singh, J. (2025). *Perspective and Challenges of Synergistic Removal of Toxic Contaminants from Effluent Using Different Treatment Techniques, Microbial Niche Nexus Sustaining Environmental Biological Wastewater and Water-Environment Nexus*, Springer, Berlin.
67. Kumari, U. (2024). *Textile Dyes and Their Impact on the Natural Environment, Dye Pollution from Textile Industry: Challenges and Opportunities for Sustainable Development*, Springer, Berlin.
68. Li, X.-F., Zhang, J.-J., and Feng, X.-Q. (2024). Adsorption–photocatalytic synergistic removal of MB by peanut shell biochar-supported TiO₂/Ce–C₃N₄ heterojunctions. *New Journal of Chemistry*, 48(39), 17321–17336.
69. Li, Z., Li, W., Wang, J., Jing, L., Li, P., Zhang, H., Fan, Y., Wang, H., Chen, Z., and Hu, J. (2024). Roles of Cocatalysts in Biomass Photo (electro) refining. *Advanced Energy Materials*, 14(42), 2401838.
70. Li, Z., Liu, D., Huang, W., Wei, X., and Huang, W. (2020). Biochar supported CuO composites used as an efficient peroxymonosulfate activator for highly saline organic wastewater treatment. *Science of the total environment*, 721, 137764.
71. Liang, L., Cai, S., Zhang, L., Sun, K., He, Z., Zhang, L., Huang, C., Long, M., Zhu, H., and Zou, B. (2024). D/A heterojunction photocatalysts interspersed onto biochar to couple photocatalysis and adsorption for visible light-responsive efficient removal of pollutants. *Journal of Alloys and Compounds*, 1005, 176093.
72. Liu, C., and Zhang, H.-X. (2022). Modified-biochar adsorbents (MBAs) for heavy-metal ions adsorption: A critical review. *Journal of Environmental Chemical Engineering*, 10(2), 107393.
73. Liu, W., Wang, X.-M., Li, D., Gao, Y., Wang, K., and Huang, X. (2025). Dominant mechanism of nanofiltration for chloride/sulfate ion separation in high salinity solutions: The quantification of pore size-influenced dielectric exclusion. *Environmental Science and Technology*, 59(11), 5848–5855.
74. Magdalane, C.M., Kaviyarasu, K., Vijaya, J.J., Sidhardha, B., Jeyaraj, B., Kennedy, J., and Maaza, M. (2017). Evaluation on the heterostructured CeO₂/Y₂O₃ binary metal oxide nanocomposites for UV/Vis light induced photocatalytic degradation of Rhodamine-B dye for textile engineering application. *Journal of Alloys and Compounds*, 727, 1324–1337.
75. Mittal, J., Arora, C., and Mittal, A. (2022). Application of biochar for the removal of methylene blue from aquatic environments. *Biomass-Derived Materials for Environmental Applications*, Elsevier, Netherlands.
76. Mukherjee, P., Sharma, R. S., and Mishra, V. (2024). Deciphering the ecological impact of azo dye pollution through microbial community analysis in water–sediment microcosms. *Environmental Science and Pollution Research*. <https://doi.org/10.1007/s11356-024-34445-w>
77. Mutlu, H., Geiselhart, C.M., and Barner-Kowollik, C. (2018). Untapped potential for debonding on demand: the wonderful world of azo-compounds. *Materials Horizons*, 5(2), 162–183.
78. Lotha, N.T., Sorhie, V., Bharali, P., and Jamir, L. (2024). Advancement in sustainable wastewater treatment: A multifaceted approach to textile dye removal through physical, biological and chemical techniques. *ChemistrySelect*, 9(11), e202304093.
79. Ning, J., Kamali, M., and Appels, L. (2024). Advances in carbonaceous promoters for anaerobic digestion processes—Functions and mechanisms of action. *Renewable and Sustainable Energy Reviews*, 202, 114640.
80. Oguanobi, N.C., Aniagor, C.O., Okoronkwo, G., Ude, C.N., Onu, C.E., and Anike, E.N. (2025). Industrial dye effluent sources, generation, and value-added products, *Engineered Biocomposites for Dye Adsorption*, Elsevier, Netherlands.
81. Oliveira, J.M.S., Sabatini, C.A., Santos-Neto, A.J.D., and Foresti, E. (2023). Broken into pieces: The challenges of determining sulfonated azo dyes in biological reactor effluents using LC-ESI-MS/MS analysis. *Environmental Pollution*, 318, 120877.
82. Oluwasina, O.O., Adelodun, A.A., Oluwasina, O.O., Duarte, H.A., and Olusegun, S.J. (2024). Experimental and computational studies of crystal violet removal from aqueous solution using sulfonated graphene oxide. *Scientific Reports*, 14(1), 6207.
83. Omoregie, I.P., Osagie, A.D., and Oritseweyinmi, O.O. (2023). Crustacean nanochitosan-based bioremediation of nanoplastic-polluted aquatic habitat: A review pursuant to SDG 6. *Scientific African*, 21, e01881.
84. Oraon, A., Prajapati, A.K., Ram, M., Saxena, V.K., Dutta, S., and Gupta, A.K. (2024). Synthesis, characterization, and application of microporous biochar prepared from Pterospermum acerifolium plant fruit shell waste for methylene blue dye adsorption: the role of surface modification by SDS surfactant. *Biomass Conversion and Biorefinery*, 14(1), 931–953.
85. Pavlenko, V., Żóltowska, S., Haruna, A., Zahid, M., Mansurov, Z., Supiyeva, Z., Galal, A., Ozoemena, K., Abbas, Q., and Jesionowski, T. (2022). A comprehensive review of template-assisted porous carbons: Modern preparation methods and advanced applications. *Materials Science and Engineering: R: Reports*, 149, 100682.
86. Periyasamy, A.P. (2024). Recent advances in the remediation of textile-dye-containing wastewater: prioritizing human health and sustainable wastewater treatment. *Sustainability*, 16(2), 495.
87. Pucciarelli, M. (2023). *Life Cycle Thinking for the*

- sustainability assessment of nanoparticles' manufacturing and applications*, University College London, London.
88. Qian, Y., Li, B., Irfan, M., Li, D., and Jiang, H.-L. (2024). Reactive oxygen species generation for catalysis and biotherapeutic applications based on crystalline porous materials. *Coordination Chemistry Reviews*, 518, 216068.
 89. Qin, Y., Li, D., Yao, T., Ali, A., Wu, J., and Yao, S. (2024). Covalent organic frameworks and related innovative materials in chiral separation and recognition. *Biomedical Chromatography*, 38(12), e6008.
 90. Qiu, B., Shao, Q., Shi, J., Yang, C., and Chu, H. (2022). Application of biochar for the adsorption of organic pollutants from wastewater: Modification strategies, mechanisms and challenges. *Separation and Purification Technology*, 300, 121925.
 91. Radoor, S., Kassahun, S.K., and Kim, H. (2024). Selective adsorption of cationic dye by κ -carrageenan-potato starch bio-hydrogel: Kinetics, isotherm, and thermodynamic studies. *International Journal of Biological Macromolecules*, 281, 136377.
 92. Rajak, P., Ganguly, A., Nanda, S., Mandi, M., Ghanty, S., Das, K., Biswas, G., and Sarkar, S. (2024). Toxic contaminants and their impacts on aquatic ecology and habitats, *Spatial Modeling of Environmental Pollution and Ecological Risk*, Elsevier, Netherlands.
 93. Ramamurthy, K., Priya, P.S., Murugan, R., and Arockiaraj, J. (2024). Hues of risk: investigating genotoxicity and environmental impacts of azo textile dyes. *Environmental Science and Pollution Research*, 31(23), 33190–33211.
 94. Ran, T., Ji, C., Zhang, Q., Wang, S., Zhang, Y., Niu, W., Wei, T., and Shi, Y. (2024). Advanced treatment and reuse of dye wastewater using thermo-irreversible on/off switch starch with disruption of dissolution/precipitation dynamic equilibrium. *Carbohydrate Polymers*, 342, 122425.
 95. Rangarajan, G., Jayaseelan, A., and Farnood, R. (2022). Photocatalytic reactive oxygen species generation and their mechanisms of action in pollutant removal with biochar supported photocatalysts: A review. *Journal of Cleaner Production*, 346, 131155.
 96. Rao, L., Jin, B., Chen, D., Jin, X., Liu, G., Huang, Z., Cao, K., Chen, F., and Huang, Q. (2024). Energy-saving CO₂ desorption from amine solution over Fe/SiO₂/biochar catalysts: Desorption performance, structure-activity relationship, and mechanism. *Chemical Engineering Journal*, 483, 149413.
 97. Rawat, S., Boobalan, T., Sathish, M., Hotha, S., and Thallada, B. (2023). Utilization of CO₂ activated litchi seed biochar for the fabrication of supercapacitor electrodes. *Biomass and Bioenergy*, 171, 106747.
 98. Rubangakene, N.O., Elwardany, A., Fujii, M., Sekiguchi, H., Elkady, M., and Shokry, H. (2023). Biosorption of Congo Red dye from aqueous solutions using pristine biochar and ZnO biochar from green pea peels. *Chemical Engineering Research and Design*, 189, 636–651.
 99. Sahu, A., and Poler, J. C. (2024). Removal and degradation of dyes from textile industry wastewater: Benchmarking recent advancements, toxicity assessment and cost analysis of treatment processes. *Journal of Environmental Chemical Engineering*, 12, 113754.
 100. Salahshoori, I., Wang, Q., Nobre, M.A., Mohammadi, A.H., Dawi, E.A., and Khonakdar, H.A. (2024). Molecular simulation-based insights into dye pollutant adsorption: a perspective review. *Advances in Colloid and Interface Science*, 333, 103281.
 101. Samaraweera, H., Alam, S.S., Nawalage, S., Parashar, D., Khan, A.H., Chui, I., Perez, F., and Mlsna, T. (2023). Facile synthesis and life cycle assessment of Iron oxide-Douglas fir biochar hybrid for anionic dye removal from water. *Journal of Water Process Engineering*, 56, 104377.
 102. Sannino, F., Allia, P., Barrera, G., Cinquegrana, A., Cirillo, C., Latte, A., Olivetti, E.S., Tiberto, P. M., and Pirozzi, D. (2024). Two alternative approaches for the magnetic adsorption of the hydrophobic dye Methylene Blue. *Journal of Molecular Liquids*, 409, 125395.
 103. Sayed, M.A., Abdelhameed, R.M., Badr, I.H., and Abdel-Aziz, A.M. (2025). Efficient adsorptive removal of hazardous congo red dye using Ce-BTC@ microcrystalline cellulose composite. *Scientific Reports*, 15(1), 19734.
 104. Selim, M.M., Tounsi, A., Gomaa, H., Hu, N., and Shenashen, M. (2024). Addressing emerging contaminants in wastewater: Insights from adsorption isotherms and adsorbents: A comprehensive review. *Alexandria Engineering Journal*, 100, 61–71.
 105. Selvaraj, V., Karthika, T.S., Mansiya, C., and Alagar, M. (2021). An over review on recently developed techniques, mechanisms and intermediate involved in the advanced azo dye degradation for industrial applications. *Journal of molecular structure*, 1224, 129195.
 106. Shafiq, M., Alazba, A.A., and Amin, M.T. (2025). Eco-friendly nanocomposite of manganese-iron and plant waste derived biochar for optimizing Pb₂⁺ adsorption: A response surface methodology approach. *Desalination and Water Treatment*, 322, 101091.
 107. Sharma, M., Sharma, S., Akhtar, M., Kumar, R., Umar, A., Alkhanjaf, A., and Baskoutas, S. (2024). Microorganisms-assisted degradation of Acid Orange 7 dye: a review. *International Journal of Environmental Science and Technology*, 21(7),

- 6133–6166.
108. Shawky, A.M., Elshypany, R., El Sharkawy, H.M., Mubarak, M.F., and Selim, H. (2024). Emerald eco-synthesis: harnessing oleander for green silver nanoparticle production and advancing photocatalytic MB degradation with TiO₂ and CuO nanocomposite. *Scientific Reports*, 14(1), 2456.
 109. Shi, J., Jiang, J., Chen, Q., Wang, L., Nian, K., and Long, T. (2023). Production of higher toxic intermediates of organic pollutants during chemical oxidation processes: A review. *Arabian Journal of Chemistry*, 16(7), 104856.
 110. Sibhatu, A.K., Weldegebrerial, G.K., Imteyaz, S., Sagadevan, S., Tran, N.N., and Hessel, V. (2022). Synthesis and process parametric effects on the photocatalyst efficiency of CuO nanostructures for decontamination of toxic heavy metal ions. *Chemical Engineering and Processing-Process Intensification*, 173, 108814.
 111. Singh, A., Kaur, S., Thakur, H., Rashi, Kashyap, S., Lyudmila, A., and Mudgal, G. (2025). Unveiling the transformative power of smart cellulosic nanomaterials: revisiting potential promises to sustainable future, *Functionalized Cellulose Materials: Sustainable Manufacturing and Applications*, Springer, Berlin.
 112. Singh, G.B., Vinayak, A., Mudgal, G., and Kesari, K.K. (2024). Azo dye bioremediation: An interdisciplinary path to sustainable fashion. *Environmental Technology and Innovation*, 36, 103832.
 113. Sornaly, H.H., Ahmed, S., Titin, K.F., Islam, M.N., Parvin, A., Islam, M.A., Faruquee, H.M., Biswas, K.K., Islam, R., and Paul, D.K. (2024). The utility of bioremediation approach over physicochemical methods to detoxify dyes discharges from textile effluents: A comprehensive review study. *Sustainable Chemistry and Pharmacy*, 39, 101538.
 114. Strelbel, A., Behringer, M., Hilbig, H., Machner, A., and Helmreich, B. (2024). Anionic azo dyes and their removal from textile wastewater through adsorption by various adsorbents: a critical review. *Frontiers in Environmental Engineering*, 3, 1347981.
 115. Sutar, S., Patil, P., and Jadhav, J. (2022). Recent advances in biochar technology for textile dyes wastewater remediation: A review. *Environmental Research*, 209, 112841.
 116. Suthar, P., and Patidar, D. (2024). Hydrothermally synthesized MoS₂ NFs toward efficient supercapacitor and fast photocatalytic degradation of MB. *Research on Chemical Intermediates*, 50(8), 3569-3595.
 117. Takhar, V., and Singh, S. (2025). Nanomaterials ROS: a comprehensive review for environmental applications. *Environmental Science: Nano*, 12, 2516–2550.
 118. Tawo, O. E., and Mbamalu, M. I. (2025). Advancing waste valorization techniques for sustainable industrial operations and improved environmental safety. *International Journal of Science and Research Archive* 14(2), 127–149.
 119. Tran, H.N., You, S.-J., and Chao, H.-P. (2017). Insight into adsorption mechanism of cationic dye onto agricultural residues-derived hydrochars: negligible role of π - π interaction. *Korean Journal of Chemical Engineering*, 34, 1708–1720.
 120. Tripathy, J., Mishra, A., Pandey, M., Thakur, R.R., Chand, S., Rout, P.R., and Shahid, M.K. (2024). Advances in nanoparticles and nanocomposites for water and wastewater treatment: A review. *Water*, 16(11), 1481.
 121. Tsauria, Q.D., Gareso, P.L., and Tahir, D. (2025). Systematic review of chitosan-based adsorbents for heavy metal and dye remediation. *Integrated Environmental Assessment and Management*, vjaf037. <https://doi.org/10.1093/inteam/vjaf037>
 122. Uddin, F. (2021). Environmental hazard in textile dyeing wastewater from local textile industry. *Celulose*, 28(17), 10715–10739.
 123. Ullah, F., Khan, Z.U.H., Sabahat, S., Aftab, M., Sun, J., Shah, N.S., Rahim, A., Abdullah, M. M., and Imran, M. (2025). Synergistic degradation of toxic azo dyes using Mn-CuO@ Biochar: An efficient adsorptive and photocatalytic approach for wastewater treatment. *Chemical Engineering Science*, 302, 120844.
 124. Waliullah, R., Rehan, A. I., Awual, M. E., Rasee, A. I., Sheikh, M. C., Salman, M. S., Hossain, M. S., Hasan, M. M., Kubra, K. T., and Hasan, M. N. (2023). Optimization of toxic dye removal from contaminated water using chitosan-grafted novel nanocomposite adsorbent. *Journal of Molecular Liquids*, 388, 122763.
 125. Wang, L., Zhang, J., Cheng, D., Guo, W., Cao, X., Xue, J., Haris, M., Ye, Y., and Ngo, H. H. (2024). Biochar-based functional materials for the abatement of emerging pollutants from aquatic matrices. *Environmental Research*, 252, 119052.
 126. Wang, W., Jin, Y., Meng, X., Yang, N., and Zhu, X. (2025). Dynamic short hydrogen-bonding network enhancing hydrophilicity in biomimetic membranes with artificial water channels for efficient removal of dyes and salts. *Angewandte Chemie*, 137(20), e202502204.
 127. Wang, X., Xia, L., Cheng, H., Li, K., Feng, W., Dai, X., and Chen, Y. (2024). Ultrasound-mediated Cu²⁺/Cu⁺ redox cycling activates peroxymonosulfate for oxygen-independent reactive X species (X= O/S) therapy. *Nano Today*, 55, 102180.
 128. Weidner, E., Karbassiyazdi, E., Altaee, A., Jesionowski, T., and Ciesielczyk, F. (2022). Hybrid metal oxide/biochar materials for wastewater

- treatment technology: a review. *ACS Omega*, 7(31), 27062–27078.
129. Wu, J. (2022). Understanding the electric double-layer structure, capacitance, and charging dynamics. *Chemical reviews*, 122(12), 10821–10859.
 130. Xie, J., Latif, J., Yang, K., Wang, Z., Zhu, L., Yang, H., Qin, J., Ni, Z., Jia, H., and Xin, W. (2024). A state-of-art review on the redox activity of persistent free radicals in biochar. *Water Research*, 255, 121516.
 131. Xie, Z.-H., He, C.-S., Zhou, H.-Y., Li, L.-L., Liu, Y., Du, Y., Liu, W., Mu, Y., and Lai, B. (2022). Effects of molecular structure on organic contaminants' degradation efficiency and dominant ROS in the advanced oxidation process with multiple ROS. *Environmental Science and Technology*, 56(12), 8784–8795.
 132. Xu, W., Qin, R., Cao, G., Qiang, Y., Lai, M., and Lu, Y. (2024). Magnetic composite photocatalyst NiFe₂O₄/ZnIn₂S₄/biochar for efficient removal of antibiotics in water under visible light: Performance, mechanism and pathway. *Environmental Pollution*, 360, 124602.
 133. Xue, Q., Lin, H., Feng, Q., Yang, Y., Dong, M., Hu, K., Song, B., Goh, P. S., and Shen, X. (2025). Synergistic photocatalysis and fenton-like process driven by a biochar-supported biochar/iron hydroxide oxide/bismuth molybdate S-type heterojunction for tetracycline degradation: Mechanistic insights and degradation pathways. *Applied Surface Science*, 679, 161277.
 134. Yadav, D., Das, S., Saharan, P., and Bhukal, S. (2026). Enhanced adsorptive removal of NAP from water using neem leaf biochar and zinc-modified nanobiochar: Isotherm, kinetic, and mechanistic investigations. *Biomass and Bioenergy*, 205, 108526.
 135. Yan, L., Song, X., Miao, J., Ma, Y., Zhao, T., and Yin, M. (2024). Removal of tetracycline from water by adsorption with biochar: A review. *Journal of Water Process Engineering*, 60, 105215.
 136. Yang, X. F., Yi, G. P., Lv, P. F., Wen, S. J., Zhao, Y. P., Jing, Z., Wang, Q., Li, B., and Tang, P. Y. (2025). Oxygen vacancy engineering of metal oxide materials for photoelectrochemical water splitting. *Electron*, 3(3), e70011.
 137. Yang, Y., Chen, Q., Zhong, X., Tan, Z., Chen, L., Han, T., Jia, B., Liu, K., Ke, G., and He, H. (2024). Photothermal effect improving the activity of spinel MnFe₂O₄ nanoparticles for the catalytic activation HCO₃⁻/H₂O₂ to achieve the degradation of dye pollutants in low-temperature condition. *Applied Surface Science*, 672, 160801.
 138. Yaseen, D., and Scholz, M. (2019). Textile dye wastewater characteristics and constituents of synthetic effluents: a critical review. *International Journal of Environmental Science and Technology*, 16, 1193–1226.
 139. Yılmaz Oral, Z. F., Kaya, M., and Kaban, G. (2024). Using celery powder in a semi-dry fermented sausage 'heat-treated sucuk': nitrosamine formation, lipid oxidation, and volatile compounds. *Foods*, 13(20), 3306.
 140. Yu, S., Zhou, J., Ren, Y., Yang, Z., Zhong, M., Feng, X., Su, B., and Lei, Z. (2023). Excellent adsorptive-photocatalytic performance of zinc oxide and biomass derived N, O-contained biochar nanocomposites for dyes and antibiotic removal. *Chemical Engineering Journal*, 451, 138959.
 141. Zhang, D., Xiong, W., Yang, D., Gao, P., Gao, C., and Li, L. (2024). Dual Fe³⁺/Fe²⁺ redox cycles boost H₂O₂ activation and enhance photooxidation behavior for degradation of tetracycline pollutants. *Journal of Materials Science: Materials in Electronics*, 35(18), 1250.
 142. Zhang, M., Ruan, J., Wang, X., Shao, W., Chen, Z., Chen, Z., Gu, C., Qiao, W., and Li, J. (2023). Selective oxidation of organic pollutants based on reactive oxygen species and the molecular structure: Degradation behavior and mechanism analysis. *Water Research*, 246, 120697.
 143. Zhang, P., Sun, M., Liang, J., Xiong, Z., Liu, Y., Peng, J., Yuan, Y., Zhang, H., Zhou, P., and Lai, B. (2024). pH-modulated oxidation of organic pollutants for water decontamination: A deep insight into reactivity and oxidation pathway. *Journal of Hazardous Materials*, 471, 134393.
 144. Zhang, Y., Lin, Y., Gan, N., Zhang, J., Wu, B., Yu, J., Matsuyama, H., and Wang, R. (2024). Angstrom-scale channels with versatile ion-membrane interactions enabling precise ion separation via electrodialysis. *AIChE Journal*, 70(10), e18519.
 145. Zhang, Y., Zhu, C., Liu, F., Yuan, Y., Wu, H., and Li, A. (2019). Effects of ionic strength on removal of toxic pollutants from aqueous media with multifarious adsorbents: A review. *Science of the total environment*, 646, 265–279.
 146. Zhao, C., Wang, B., Theng, B.K., Wu, P., Liu, F., Wang, S., Lee, X., Chen, M., Li, L., and Zhang, X. (2021). Formation and mechanisms of nano-metal oxide-biochar composites for pollutants removal: A review. *Science of the total environment*, 767, 145305.
 147. Zheng, A.L.T., Lih, E.T.Y., Hung, Y.P., Boonyuen, S., Al Edrus, S.S.O., Chung, E.L.T., and Andou, Y. (2025). Biochar-based electrochemical sensors: a tailored approach to environmental monitoring. *Analytical Sciences*, 41, 715–735.